Environmental Pollution 345 (2024) 123431

Contents lists available at ScienceDirect

Environmental Pollution

journal homepage: www.elsevier.com/locate/envpol

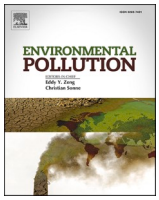

Enhancing hydro-epidemiological modelling of nearshore coastal waters with source-receptor connectivity study☆

Man Yue Lam *, Reza Ahmadian

School Of Engineering, Cardiff University, Cardiff, Uk

ARTICLE INFO

Keywords:
Water quality modelling
Faecal indicator organisms
Source-receptor connectivity
Swansea bay
Microbe decay models
Impulse response function

ABSTRACT

Faecal Indicator Organism (FIO) concentrations in nearshore coastal waters may lead to significant public health concerns and economic loss. A three-dimensional numerical source-receptor connectivity study was conducted to improve the modelling of FIO transport and decay processes and identify major FIO sources impacting sensitive receptors (source apportionment). The study site was Swansea Bay, UK and the effects of wind, density, and tracer microbe (surrogate FIO) decay models were investigated by comparing the model simulations to microbial tracer field studies. The relevance of connectivity tests to source apportionment was demonstrated by hindcasting FIO concentration in Swansea Bay with the identified FIO source and the Impulse Response Function (IRF) in Control System theory. This is the first time the IRF approach has been applied for FIO modelling in bathing waters. Results show the importance of density, widely ignored in fully mixed water bodies, and the potential for biphasic decay models to improve prediction accuracy. The microbe-carrying riverine freshwater, having a smaller hydrostatic pressure, could not intrude on the heavier seawater and remained in the nearshore areas. The freshwater and the associated tracer microbes then travelled along the shoreline and reached bathing water sites. This effect cannot be faithfully modelled without the inclusion of the density effect. Biphasic decay models improved the agreement between measured and modelled microbe concentrations. The IRF hindcasted and measured FIO concentrations for Swansea Bay agreed reasonably, demonstrating the importance of connectivity tests in identifying key FIO sources. The findings of this study, namely enhancing hydro-epidemiological modelling and highlighting the effectiveness of connectivity studies in identifying key FIO sources, directly benefit hydraulics and water quality modellers, regulatory authorities, water resource managers and policy.

1. Introduction

Water quality in nearshore coastal waters is a global concern, given that coastal waters are crucial for human activities such as recreation, aquaculture, and economic revenue. Water contaminants may lead to significant public health concerns and economic losses, e.g. consumption of contaminated shellfish, reduced tourism, and swimming-related illnesses (DeFlorio-Barker et al., 2018; Bussi et al., 2017; Given et al., 2006; Weiskerger and Phanikumar, 2020). Faecal Indicator Organisms (FIOs), one of the contaminants, are highly correlated with illnesses such as gastrointestinal infections and eye infections (Pruss, 1998; Pandey et al., 2014). For European countries, the European Union (EU) revised Bathing Water Directive (rBWD, European Commission, 2006) requires two FIO species in bathing water sites to be below given levels. However, the routine single-point and low-frequency rBWD monitoring scheme does not address diurnal (Wyer et al., 2018) and spatial (King, 2019) variations of FIO concentration. Also, stormwater runoffs and Combined Sewage Overflows (CSOs) increase nearshore FIO concentration by 1,000 % to 10,000 % for several hours or days (e.g. Ahn et al., 2005; Passerat et al., 2011). More stormwater runoffs and CSOs are expected in future due to climate change, population growth, and urbanisation (Semadeni-Davies et al., 2008; Jalliffier-Verne et al., 2017). In addition, FIO monitoring does not provide (i) predictions of future FIO concentration and (ii) an understanding of the transport and fate of FIOs in coastal waters, which are important for protecting public and environmental health and for water companies to improve their energy efficiency. Hydro-epidemiological models (e.g. Lee and Qu, 2004; Schippmann et al., 2013; Harris et al., 2004; Gao et al., 2013) are

☆ This paper has been recommended for acceptance by Sarah Harmon.

* Corresponding author.
E-mail addresses: lamm7@cardiff.ac.uk (M.Y. Lam), Ahmadianr@cardiff.ac.uk (R. Ahmadian).

https://doi.org/10.1016/j.envpol.2024.123431
Received 31 August 2023; Received in revised form 17 December 2023; Accepted 21 January 2024
Available online 30 January 2024

indispensable tools for understanding the transport and fate of FIOs as well as evaluating water quality improvement strategies. This research tests and improves different components of hydro-epidemiological modelling, especially density effect and FIO decay models, with connectivity tests. The effectiveness of connectivity tests in identifying key FIO sources is also demonstrated.

While the effect of density on estuaries and water quality has been studied in the literature (e.g. Geyer et al., 2004; Ji, 2008; Bedri et al., 2013; Gaeta et al., 2020), surprisingly, this effect has rarely been considered for FIO modelling in fully mixed water bodies and bathing water sites. In addition, two-dimensional models neglecting the density effect are widely used for FIO source-receptor connectivity research and water quality management (Ahmadian et al., 2013; Abu-Bakar et al., 2017; King et al., 2021). FIO decay in coastal environments depends on numerous environmental factors such as irradiation, salinity, and turbidity (e.g. Bowie et al., 1985; Crane and Moore, 1986; Abu-Bakar et al., 2017; Weiskerger and Phanikumar, 2020). Such a decay process is usually represented by a first-order degradation model with variable decay rates. Several studies of FIO decay in natural waterbodies suggest a biphasic decay model (Bowie et al., 1985; Crane and Moore, 1986) to represent (i) the decay rate when the FIOs are first injected into the waterbodies; and (ii) the one after the FIOs have adapted to the waterbodies. Accurate representations of these effects are important for hydro-epidemiological modelling of FIOs.

This research aims to improve hydro-epidemiological modelling to better simulate and understand the fate and transport of FIOs in nearshore coastal waters. This was achieved by the following objectives: (i) investigating the key process(es) affecting FIOs transport, (ii) improving the simulation of microbe (surrogate FIO) decay models, and (iii) assessing the effectiveness of connectivity tests in identifying key FIO sources with the Impulse Response Function (IRF) approach. The key methodology is numerical connectivity tests. Hydro-epidemiological models have been tested by comparing modelled and measured FIO concentrations, such as total coliform, *E. coli*, and *Enterococci* in coastal waters, lakes, and rivers (e.g. Hipsey et al., 2008; Liu et al., 2015). Nevertheless, the uncertainty of FIO sources for any given waterbodies adds uncertainty to the test results. Such an uncertainty can be avoided by conducting connectivity tests, in which the source locations and concentrations were known. In a connectivity test, natural dyes or tracer microbes which are not naturally present in a waterbody are released at potential source locations (e.g. river inflows) and are measured at potential sensitive receptors. The injected dynes or tracer microbes are seen as surrogate FIOs, yet with known injection locations and concentrations. Connectivity between sources and receptors is easily identified since the tracer microbes are identifiable from other bacteria that are naturally present in the waterbody (e.g. Varlamov et al., 1999; Isobe et al., 2009; Wyer et al., 2010, 2014; Andruszkiewicz et al., 2019). The effectiveness of connectivity test to identify FIO sources (i.e. source apportionment) is also demonstrated through hindcasting FIO concentrations with the connectivity test results and the Impulse Response Function (IRF) in Control System theory. IRF has been applied in control systems (Schwarzenbach and Gill, 1992; Ogata, 2015) and transient defect detection in pipelines (e.g. Liou, 1998; Ferrante and Brunone, 2003; Wang et al., 2020), but this is the first time IRF approach is applied for FIO modelling in bathing waters.

2. Materials and methods

Fig. 1 shows the flow chart of the research methodology. Three-dimensional (3D) hydro-epidemiological models were developed to simulate the connectivity test conducted in Swansea Bay, UK, in year 2012 as part of the "Smart Coasts – Sustainable Communities (SCSC)" research project (Wyer et al., 2014). Effects of density and microbe (i.e. surrogate FIO) decay model were evaluated against the field data, and FIO sources in the test site were identified. To verify the identified sources, the *E. coli* concentrations measured at the test site in the year 2011 from the same SCSC project were hindcasted with the IRF approach, the identified FIO source locations and the measured source concentrations in the corresponding measurement period.

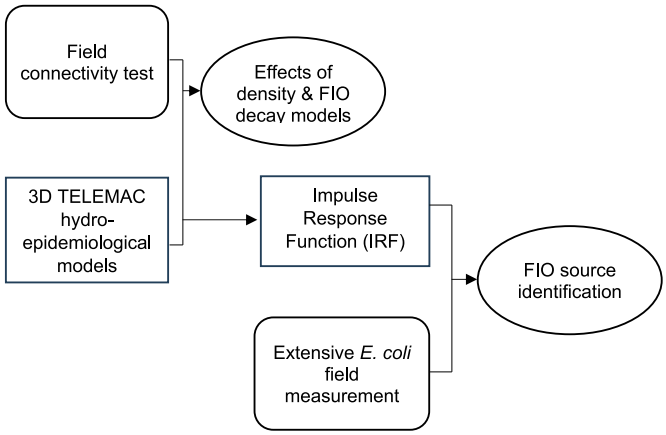

Fig. 1. Flow chart of the modelling study. Rectangles represent modelling or computation tasks; round-cornered rectangles represent data from the SCSC project; circles represent conclusions from modelling or computation tasks.

2.1. The test site: Swansea Bay, UK

Swansea Bay is located in the Bristol Channel on the South Wales Coast, UK. Bristol Channel and Severn Estuary have a typical tidal range of about 12–14 m during high spring tides, which is the second highest in the world (British Crown and OceanWise Ltd., 2015). The Bay is subjected to FIO sources including River Tawe, Neath and Afan (flow rate >1 m^3/s), streams and drains (flow rates <1 m^3/s), and three sewage treatment work (STW) effluents. Swansea Bay is a well-mixed waterbody (Uncles, 1981; Evans et al., 1990; Ahmadian et al., 2013) where temperature and salinity variations through the water column are negligible. Nevertheless, horizontal salinity gradients are present (Collins and Banner, 1980). Swansea Bay was chosen because of the availability of data and its relevance to swimmers. FIO data and data for stream flows, tide levels, meteorology and water quality were available from the SCSC research project (Wyer et al., 2013). There are several popular beaches along the shoreline, including Swansea Beach and Aberafan Beach. A better understanding of the sources, transport, and fate of FIOs enables the improvement of water quality in this area and protects public health. Figure SI-1 shows Swansea Bay and the FIO sources for the Bay.

2.2. Source-receptor study in Swansea Bay, UK

Fig. 2 shows the tracer microbe release and sampling locations for the connectivity test in the SCSC project (Wyer et al., 2014). Four tracer microbe species were released at four release points at about 10:00, 11 Mar 2012. Table 1 shows the microbe species and quantities released at each point. *E. Cloacae*, *MS2 coliphage*, and *S. marcescens* were measured in plaque-forming units (pfu), yet *B. atrophaeus* was measured in colony-forming units (cfu). The tracer microbes were sampled at four bathing water sites: (i) Swansea; (ii) Crymlyn Burrows; (iii) Aberafan; and (iv) Margam Sands. Single point sampling for each location was prohibited by the large tidal flats, up to 1,500 m from shore, caused by the large tidal range and sloping beaches in the Bay. Therefore, the sampling points were moved across the shoreline to achieve a minimum water depth for sampling as shown by the yellow crosses in Fig. 2. Readers are referred to Wyer et al. (2014) for the detailed field test procedures.

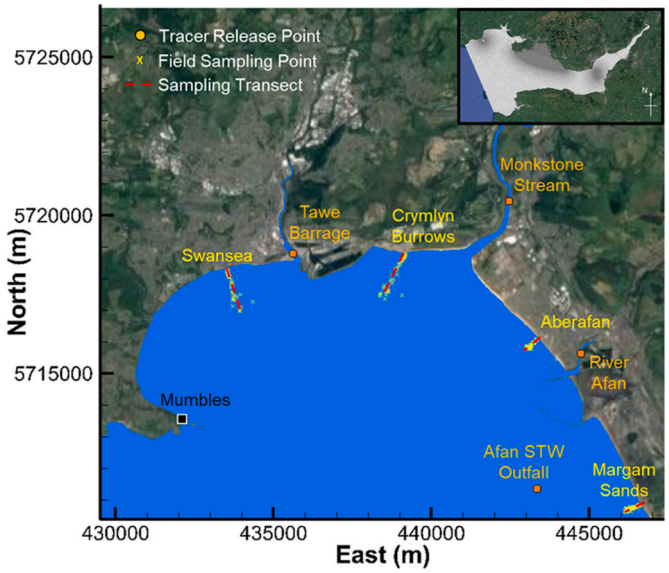

Fig. 2. Tracer microbe release points and sampling points in the field connectivity tests, and the sampling transects in the numerical models.

Table 1
Release locations of different microbe species in Swansea Bay. *E. Cloacae*, *MS2 coliphage*, and *S. marcescens* were measured in plaque-forming units (pfu), yet *B. atrophaeus* was measured in colony-forming units (cfu).

Release location	Microbe species	Count (pfu or cfu)
Tawe Barrage	*E. cloacae*	2.00×10^{16}
Monkstone Stream	*MS2 coliphage*	3.25×10^{17}
River Afan	*S. marcescens*	2.25×10^{16}
Afan STW Outfall	*B. atrophaeus*	1.75×10^{14}

2.3. The model setup

The study was modelled with the open-source finite-element TELEMAC-3D hydrodynamic solvers (Leroy, 2019). Although stratification is not important for the Bay, the small vertical density difference might influence the horizontal transport of salinity and microbes. Therefore, 3D models were applied to ensure the representation of this effect. The solvers can simulate the buoyancy effect, and models with and without the buoyancy effect were developed. The governing equations used in TELEMAC-3D are:

$$\frac{\partial u_i}{\partial x_i} = 0 \quad [1]$$

$$\frac{\partial u_i}{\partial t} + u_j\frac{\partial u_i}{\partial x_j} = -\frac{1}{\rho}\frac{\partial p_h}{\partial x_i} - \frac{1}{\rho}\frac{\partial p_d}{\partial x_i} + \frac{\partial}{\partial x_j}\left(\nu_E\frac{\partial u_i}{\partial x_j}\right) + G_i + F_i \quad [2]$$

$$\frac{\partial C}{\partial t} + u_j\frac{\partial C}{\partial x_j} = \frac{\partial}{\partial x_j}\left(\kappa_E\frac{\partial C}{\partial x_j}\right) + Q \quad [3]$$

$$p_h = g\rho(\eta - x_3) + p_{atm} + g\rho\int_{x_3}^{\eta}\frac{\Delta\rho}{\rho}dx_3 \quad [4]$$

$$\frac{\partial \eta}{\partial t} + \frac{\partial \overline{u_j}}{\partial x_j} = 0 \quad [5]$$

where x_i are the spatial coordinates in which x_3 is the vertical coordinate; t is time; u_i is the flow velocity along direction x_i; p_h and p_d are hydrostatic and dynamic pressures; C is the concentration of a scalar (e.g. salinity or microbe); For clarity, C_{Sal} is salinity and C_m is microbe concentration; Q is a source/decay term; g is the gravitational acceleration and $G_i = (G_1, G_2, G_3) = (0, 0, g)$ is a gravitational force term; F_i is a contact force (e.g. friction) term along direction x_i; η is surface elevation; p_{atm} is atmospheric pressure; ρ is reference density and $\Delta\rho$ is density difference; the overline in Equation [5] denotes depth-averaged values. Equation [1–2] are the mass and momentum equations; Equation [3] is the transport of scalars; Equation [4] is the hydrostatic pressure with buoyancy effect; Equation [5] is the kinematic boundary condition at the free surface. The TELEMAC-3D solver models buoyancy by expressing $\frac{\Delta\rho}{\rho}$ as a function of scalars, denoted by f_b. In this work, $\frac{\Delta\rho}{\rho} = 0$ (no buoyancy) and $\frac{\Delta\rho}{\rho} = f_b(C_{Sal})$ (buoyancy is uniquely dependent on salinity) were applied. $\nu_E = \nu + \nu_T$ is effective viscosity and ν and ν_T are molecular and turbulence viscosities. Turbulence models were needed to represent the effect of turbulence on the flow and contaminant transport. The Smagorinski (1963) turbulence model was applied as it has been recommended for large-scale marine areas (Gourgue et al., 2013; Lang et al., 2014; Bedri et al., 2015) and has previously shown good performance in Severn Estuary and Bristol Channel (Guo et al., 2020; King et al., 2021).

The horizontal numerical mesh was adopted from King et al. (2021) for the Bristol Channel and Severn Estuary, UK as shown in the inset of Fig. 2 and Figure SI-2. A tidal water level series obtained from the National Oceanography Centre Continental Shelf Model (CS3; NOC, 2018) were imposed along the outer Bristol Channel boundary. A Coriolis coefficient $f = 2\pi\sin(\theta) = 1.13601 \times 10^{-4}\ rad/s$ given the latitude $\theta = 51.38^{\circ}$ was applied since the Coriolis effect was shown to slightly improve model results (King, 2019). The model domain was extended up to River Tawe and to the tidal limits of Rivers Afan and Neath to include the momentum effect of river discharges (King, 2019). Since the bay is fully mixed, freshwater input from rivers is the main source of the density gradient. The horizontal element size was about 1,000 m near the outer Bristol Channel and was refined to about 50 m in Swansea Bay because the grid-dependence study by King et al. (2021) showed that a 50 m grid size for Swansea Bay was sufficient. For models with the density effect, 10 vertical layers were used to capture possible, though weak, vertical density gradients. For models without the density effect, 5 vertical layers were used (King et al., 2021). The resulting 3D meshes consisted of 712,665 nodes and 1,125,760 elements for 5 vertical layers and 1,425,330 nodes and 2,532,960 elements for 10 vertical layers. The bottom friction was modelled with the Manning's formula (Chow, 1959) with a constant Manning coefficient $n = 0.025$ throughout the model domain following King et al. (2021). The inflows to Swansea Bay were represented by 3 boundary conditions and 12 point sources as shown in Figure SI-3. Since the microbe tracers studied did not exist in the environment apart from being injected artificially through the field study, only the water flow rates (i.e. not the FIOs or tracer microbes) at the inflows were included in the model. Flow rate data of River Tawe, Neath and Afan obtained from National River Flow Achieve (NRFA, https://nrfa.ceh.ac.uk/) on 8–13 Mar 2012 were imposed as boundary conditions. Other streams, drains and STW effluents were imposed as point sources. The available flow rate data of these sources were not measured at the time when the connectivity test was conducted, thus these flows during the test period were deduced from the time when data were available. For streams, drains, Swansea STW and Afan STW effluents, the minimum flow rates from the SCSC project data during 12–21 Jul 2011, which may represent the dry-weather flow rates, were imposed. For the Tata effluent, the average flow rate obtained from the SCSC project during 12–21 Jul 2011 was imposed. The minimum flow rate approach was not suitable for Tata effluent since the minimum flow rate was zero. Hourly mean wind data at the Mumbles obtained from the Met Office MIDAS database, as shown in Fig. 2, were used.

Table 2 shows the test cases in this study. The simulation Baseline was a 3D simulation with no effects of wind, density, and microbe decay, forming a baseline for comparison. Investigating the main processes affecting FIO transport was one of the main objectives of the study. Therefore, the effect of wind under no density effect was studied and

Table 2
Source-receptor connectivity models developed.

Name	Wind	Density	T_{90} (hr)
Baseline	No	No	No decay ($T_{90}\rightarrow\infty$);
Wind	Yes	No	No decay ($T_{90}\rightarrow\infty$);
Sal	No	Yes	No decay ($T_{90}\rightarrow\infty$);
SalWind	Yes[a]	Yes	(i) No decay ($T_{90}\rightarrow\infty$); (ii) Constant T_{90} = 30 h; (iii) Biphasic decay rate

[a] Wind effect was only imposed on the test simulations but not the precursor runs.

referred to as "Wind". The simulations referred to as "Sal" and "SalWind" studied the effect of density (i.e. salinity) with and without wind. Since SalWind was the simulation that included the widest environmental conditions and had the most promising results, for brevity, the effect of microbe decay models was only reported for SalWind. The decay model tested includes (i) no decay; (ii) a constant decay rate T_{90} = 30 *hr*; and (iii) biphasic decay rates. The microbe decay rates are further discussed in section 2.4. The simulations without salinity were cold-started. The simulations with salinity were warm-started from the salinity condition prepared from a precursor run. In the precursor run, the initial salinity and the salinity at the tidal boundary were set to be 34 kg/m^3 (Collins and Banner, 1980). A salinity of 0 kg/m^3 (freshwater) was imposed on the river boundaries and the stream, drain and STW sources. This was mainly due to the absence of measurements in the field studies conducted prior to this research. Although this assumption is expected not to affect the main conclusions, it is important that salinity is measured, and accurate value is included in modelling studies. The salinity in the Bay was diluted by the freshwater inflows once the precursor run was started. The precursor run was conducted for a simulation time of 20.8 days to ensure that the salinity concentrations were stationary before the injection of the tracer microbes as shown in Figure SI-5. After the precursor run, the model runs Sal and SalWind started and numerical tracer microbes were released at the same time and release points as in the field experiment. The tracers were released during an ebb tide around a spring tide condition with a tidal range of around 10 m as shown in Figure SI-6. The wind speed immediately after the injection of tracer microbes (10:00, 11 Mar 2012) is relatively low (less than 5 m/s within 10:00, 11 Mar – 13 Mar 2012). A numerical sampling technique that represents the transect approach in section 2.2 is desirable. Applying the field sampling point coordinates to the models was not realistic because of the inaccurate modelling of the wet-dry interface (Medeiros and Hagen, 2013). In the models, the field sampling points were represented by sampling transects shown in Fig. 2; tracer concentrations were sampled along the transects at points where the water depths were approximately equal to 1 m. The numerical implementation of the sampling method is shown and explained in Figure SI-7. The model was calibrated in King et al. (2021) and validated against an Acoustic Doppler Current Profiler (ADCP) survey in Swansea Bay (EMU Limited, 2012; also reported in King et al., 2021) at points L1-L5, and the field salinity data obtained in the SCSC research project (Ahmadian et al., 2013) at points SV1 and SV2 shown in Figure SI-8.

2.4. The microbe decay models

The tracer microbes are known to decay in the coastal environment (e.g. Bowie et al., 1985; Crane and Moore, 1986; Abu-Bakar et al., 2017; Weiskerger and Phanikumar, 2020) and the decay is commonly represented by a first-order degradation model:

$$C_m(t) = C_{m0}\exp(-kt) \quad [6]$$

where $C_m(t)$ is concentration with respect to time t; C_{m0} is initial concentration. k is usually represented in terms of T_{90} values (Schnauder et al., 2007), i.e. the time required for microbe concentration to reduce by 90 %. Several studies of microbe decay in natural waterbodies suggest a biphasic decay model (Bowie et al., 1985; Crane and Moore, 1986). An equation for the model is:

$$C_m(t) = C_{m0}\exp(-k_1 t);\ 0 \le t < t_t \quad [7]$$

$$C_m(t) = C_{m1}\exp[-k_2(t-t_t)];\ t \ge t_t \quad [8]$$

where k_1 and k_2 are the decay rates for the first and second phases respectively; t_t is the time of transition from the first to the second phase; $C_{m1} = C_{m0}\exp(-k_1 t_t)$ is the concentration after the first decay phase. Usually, the first phase has a higher decay rate than the second one for FIOs such as *E. coli*, *Enterococci,* and coliform (Rogers et al., 2011; Zhang et al., 2015), but there are environmental conditions under which faecal bacteria decay slower, or even grow, in the first phase (Perkins et al., 2016; Mattioli et al., 2017). Though interesting, understanding the processes behind the observed biphasic bacteria decay is beyond the scope of this research. While the decay rates are known to depend on factors such as temperature, irradiation, turbidity, and salinity (Byappanahalli et al., 2012; Weiskerger and Phanikumar, 2020), this study assumes constant values of k, k_1 and k_2 following the numerical tracer study in Abu-Bakar et al. (2017). In this study, the following decay models were tested: (i) conserved tracer ($T_{90}\rightarrow\infty$); (ii) constant T_{90} = 30 *hr*; and (iii) biphasic decay models with two T_{90} values. The transition time was set to be t_t = 90 *hr* from the start of the model runs. Since this study focuses on source connectivity tests in which free-living tracer microbes (i.e. microbes not attached to sediment particles) were introduced into the waterbody, sediment modelling (Ahmadian et al., 2010; Huang et al., 2015; Huang et al., 2018) was not considered as a part of this study.

2.5. FIO source identification with Impulse Response Function

The relationship between microbe (surrogate FIO) sources and receptors is represented by a system which accepts inputs and produces outputs. The mathematical representation of this system is:

$$y[k] = \sum_{h=0}^{\infty} x[k-h]w[h] \quad [9]$$

where $y[k]$ is system output; $x[k]$ is system input; $w[h]$ is the IRF of the system, representing the relationship between microbe sources and receptors in Swansea Bay UK; squared brackets denote discrete time series; k and h represent the k-th and h-th data points in the respective time series. $k-h$ represents the lag between the k-th and h-th data points. In this study, the microbe sources for the Swansea sampling transect (the receptor) were identified among the four microbe release locations. Since the microbes were surrogate FIOs, the FIO concentration at the receptor was the superposition of the microbe from the four sources. Therefore, Equation [9] was decomposed into four components:

$$y[k] = \sum_{n=1}^{4}\left[\sum_{h=0}^{\infty} x_n[k-h]w_n[h]\right] \quad [10]$$

where $w_n[h], h = 1,2,3,4$ were the IRFs relating the four respective bacteria sources, namely (i) River Tawe, (ii) Monkstone Stream, (iii) River Afan and (iv) Afan STW outfall, and the receptor; $x_n[k]$ were the number of microbes injected at the four sources respectively. $w_n[h]$ was estimated between potential sources x_n and the receptor y as in Fig. 3a. Key sources for the receptor were identified by comparing the magnitudes of w_n. Then the *E. coli* concentration at the receptor y_H during Aug–Sep 2011 was hindcasted by applying the *E. coli* input in the year 2011 at the identified source x_H (data from the SCSC project) to $w_H[h]$, the IRF for the identified source. to hindcast the as shown in Fig. 3b. The hindcast results were compared against the measured *E. coli* at the Swansea transect during Aug–Sep 2011 in the SCSC project. Additional hydro-epidemiological models were not needed for the hindcasting.

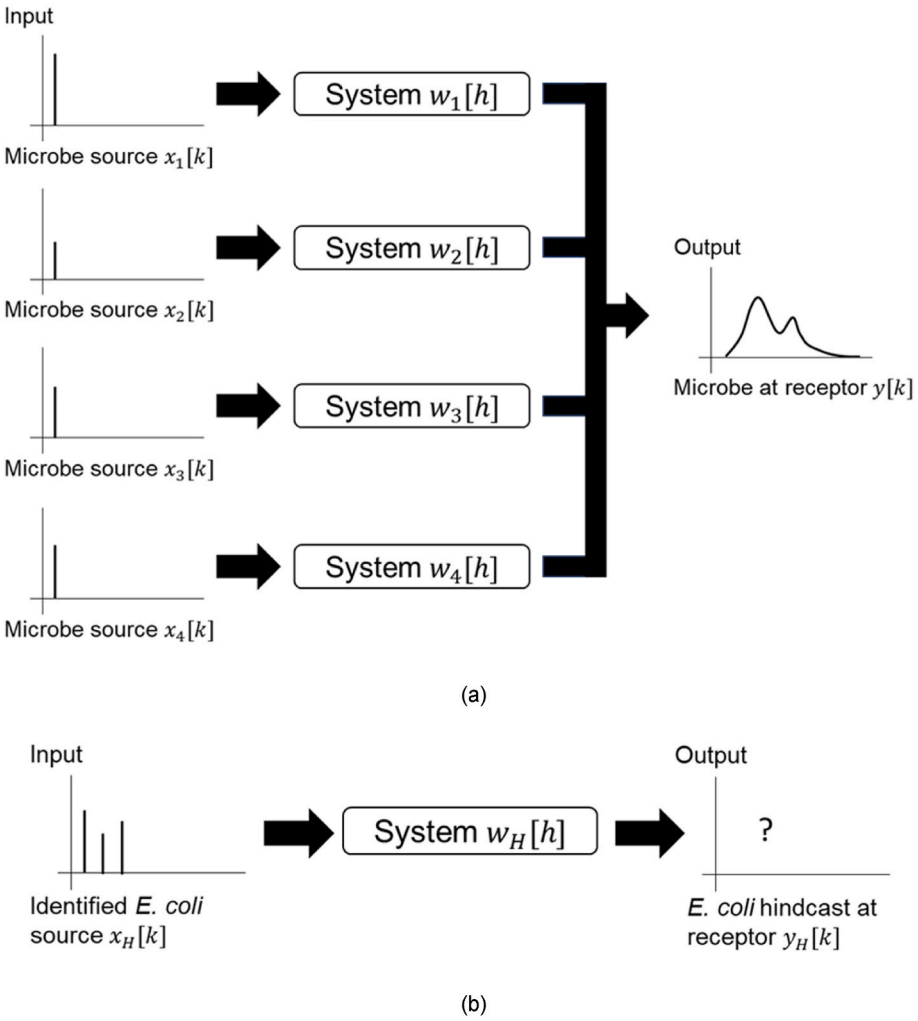

Fig. 3. (a) The transfer between microbe sources and the receptor in the connectivity test; (b) the transfer between *E. coli* at the identified source and the receptor in the hindcasting.

3. Results and discussion

3.1. Model validation

The modelled water depth and depth-averaged velocity were validated with an ADCP survey in Jul–Sep 2012. Because the field sampling period was not the same as the modelled period, the measured data that corresponds to the tidal phase and spring/neap cycle of the modelled period were selected to compare to the modelled results. The maximum and minimum RMSEs for water depth among L1-L5 were 0.3556 m and 0.3283 m, approximately 5 % of the tidal range. The errors of velocity magnitude at L2-L5 were below 12 % of the velocity range, while the error at L1 was 22 % of the velocity range. The higher modelling error at L1 might be caused by the island wake flow around the Mumbles, which may not be accurately represented in the models. The modelled vertical salinity profiles at points SV1 and SV2 were compared to the field salinity data obtained in Sep 2011 (Ahmadian et al., 2013). The measured and modelled salinity sampled at the same tidal phase, with the high tide at the Mumbles defined as 0°, well agreed as shown in Figure SI-9. The modelled salinity was shown relatively constant across the depth, which is consistent with previous studies (Uncles, 1981; Evans et al., 1990; Ahmadian et al., 2013). The modelled tracer microbe concentration was also uniform across the depth as shown in Figure SI-10. Therefore, field-measured tracer microbe concentrations at each site were compared to the modelled depth-averaged tracer concentrations from here onwards.

3.2. Effect of wind and salinity on tracer microbe transport

Models with conservative tracers (i.e. no microbe decay) were evaluated against the field measurement to study the impacts of different drivers of microbe transport. Fig. 4 shows that the models

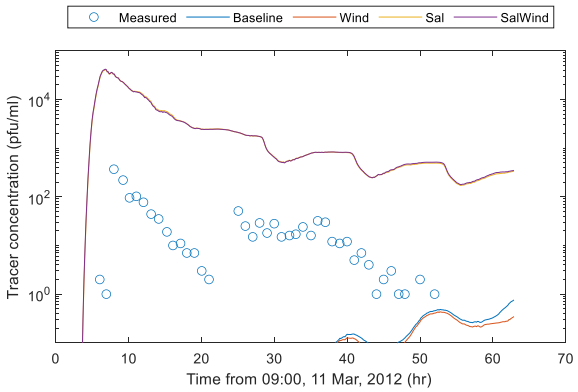

Fig. 4. Measured and modelled *S. marcescens* concentrations (released at River Afan) sampled at the Aberafan transect.

including the density effect agreed better with the field measurement at the initial tracer arrival stage. Results also show that the effect of wind is not important in this study. This could be due to the low wind speed during the tests (less than 5 m/s within 10:00, 11 Mar – 13 Mar 2012) and should be studied further in future studies. After the arrival stage, the models did not reproduce the measured microbe decay, because microbe decay models were not included in these simulations. The effect of microbe decay rates is discussed in section 3.3. Figure SI-11 shows similar observations at other transects.

The impact of density on the transport of tracers is illustrated in Fig. 5. The released microbes travelled along the shore in model SalWind but not in models without salinity. The microbes were released in the river and were mixed and transported with the fresh water. When the density effect was modelled, the fresh and lighter river water and the associated microbes tended to float on top of the seawater. The well-mixed Bay prevented vertical stratification, but a vertically well-mixed and lighter freshwater column was formed near the river outlet. The lighter freshwater column had a lower hydrostatic pressure compared to the seawater and could not intrude into the seawater, forming a freshwater-seawater interface. The freshwater was retained shoreward of this interface and travelled along the shore, reaching the Aberafan site. Models without density effect did not capture this phenomenon. The observed effect of density on contaminant transport is consistent with other studies on nearshore coastal waters (Geyer et al., 2004; Bedri et al., 2013; Gaeta et al., 2020). This highlights the importance of using 3D models including the density effect when modelling contaminants in coastal areas and could explain the discrepancies between measured and predicted results in the absence of such a modelling approach.

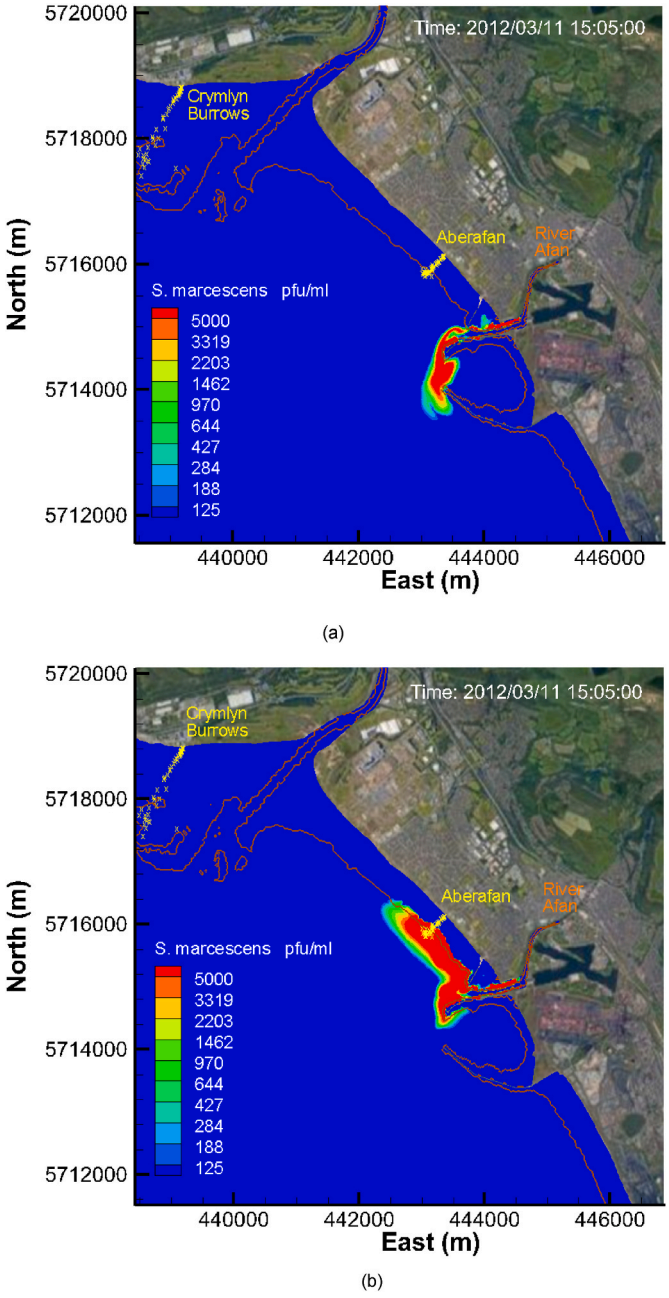

Fig. 5. Transport of *S. marcescens* (released at River Afan) for models (a) Wind, and (b) SalWind. No decay model was applied to the microbe. Brown lines illustrate the wet/dry interface (water depth = 0.02 m). Yellow crosses represent field sampling points. The contour intervals were exponentially scaled. (For interpretation of the references to colour in this figure legend, the reader is referred to the Web version of this article.)

3.3. Effect of microbe decay models

A comparison of the measured and predicted microbe concentrations using different decay models is shown in Fig. 6. While the decay model with $T_{90} = 30\ hr$ improved the tracer concentration prediction only at a later stage, the biphasic decay models improved the prediction at both the initial and later stages. Different microbe species were released at the release locations and different decay rates could be associated with different microbe species as shown in Figure SI-12. For instance, the decay rates for *E. cloacae* and *MS2 coliphage* were set to $T_{90,1} = No\ Decay$ and $T_{90,2} = 30\ hr$ while the decay rates for *S. marcescens* were $T_{90,1} = 5\ hr$ and $T_{90,2} = 30\ hr$. Unfortunately, the field data were not sufficient to validate the calibrated decay rates. In addition, this study was not focused on finding the most accurate decay rates for this case study. Improved decay rates could be found by calibrating and validating biphasic decay using RMSE between the measured and predicted concentrations. The use of biphasic decay models improved the prediction when the tracers first arrived at the transects. The calibrated tracer decay rates in this research ($T_{90} = 0 - 30\ hr$) were of a similar order of magnitude to the tracers in Abu-Bakar et al. (2017) and FIO decay rates in Ahmadian et al. (2013). The similarity in decay rates of the tracer microbes and FIOs suggests the relevance of this research to FIO concentrations in bathing water sites, while further research is needed to discover the relationship between the decay rates of the selected tracer microbes and FIOs. The results show the potential for biphasic decay models to improve microbe concentration prediction, and more sampling points are needed for microbe decay model calibration in future source-connectivity field studies and further studies on microbe decay.

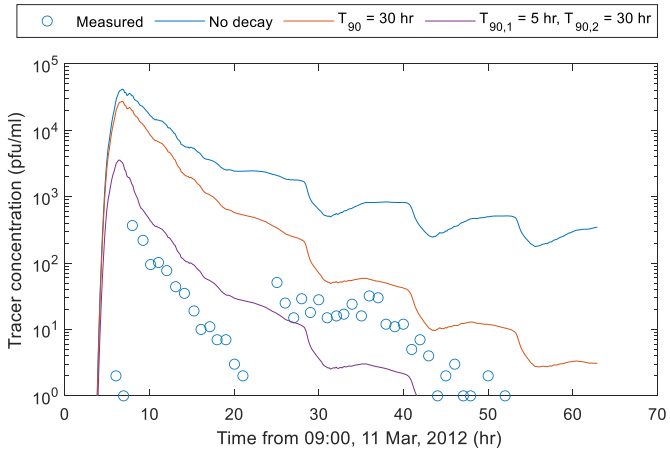

Fig. 6. Measured and modelled microbe concentrations with different decay rates in SalWind. The microbe species and sampling locations were *S. marcescens* (released at River Afan) sampled at the Aberafan transect.

4. Identifying FIO key sources using impulse response function

Equation [10] was applied between each of the four tracers and the Swansea transect (the receptor) to determine w_n. Results showed that Tawe River was the main source of microbe at the receptor since the resulting IRFs from the Tawe River release point were at least 10 times higher than other release points as shown in Figure SI-13. Therefore, only the Tawe River release point and the corresponding IRF were used in the *E. coli* concentration hindcast. Fig. 7 shows that the hindcasted and measured *E. coli* concentration agreed reasonably given (i) the difference in seasons (spring versus summer) and (ii) the potential difference in decay rates of the tracer microbe *E. cloacae*. and *E. coli*. Hindcast results for other periods within Aug–Sep 2011 were shown in Figure SI-14. The IRF-constructed *E. coli* concentration did not reproduce the measured inter-day variation of *E. coli* concentration, but the same inability was reported for other hydro-epidemiological models (Bedri et al., 2013, 2014; King et al., 2021). Further research on FIO decay rates and the FIO transport, e.g. nearshore FIO dynamics (Ge et al., 2012; Medeiros and Hagen, 2013), is necessary to improve the accuracy of hydro-epidemiological modelling and microbe prediction. This research shows the potential of using the source-receptor connectivity test for source apportionment and FIO concentration prediction.

5. Conclusions

This research aims to improve hydro-epidemiological modelling to better simulate and understand the fate and transport of FIOs in nearshore coastal waters. This was achieved by the following objectives: (i) investigating the key process(es) affecting FIO transport, (ii) improving the simulation of microbe (surrogate FIO) decay models, and (iii) assessing the effectiveness of connectivity tests in identifying key FIO sources with the IRF approach. Numerical tracer microbe studies, which include releasing microbes (surrogate FIOs) which do not exist naturally in the environment, were conducted for Swansea Bay, UK to enhance hydro-epidemiological modelling of FIOs and source apportionment. Numerical tracer microbes were released at potential contaminant sources and sampled at key receptors. Effects of density and microbe decay models on modelling accuracy were studied under controlled release of microbe sources. FIO sources for the receptors were also identified. To demonstrate the relevance of connectivity study and source apportionment, the model results were applied to hindcast FIO concentration in the Swansea transect by invoking the IRF in Control System theory. It is the first time the IRF approach has been applied for FIO modelling in bathing waters. Density was shown important for FIO transport despite the vertically well-mixed coastal water. The lighter freshwater had a smaller hydrostatic pressure compared to the heavier seawater. The freshwater thus could not intrude on the seawater and travelled along the shoreline. The tracer microbes were advected with the freshwater once they were released. This illustrates the importance of using models including the density effect when modelling contaminants in coastal areas. Biphasic decay models were also shown to improve the agreement between measured and modelled microbe concentrations. Nevertheless, the decay rates need calibration because microbe decay is a complex process which depends on a myriad of factors such as microbe species, temperature, and irradiation. The IRF hindcasted FIO concentration agreed with the measured concentration reasonably, demonstrating the importance of connectivity tests in water quality prediction. The findings of this study, namely enhancing hydro-epidemiological modelling and highlighting the effectiveness of connectivity studies in identifying key FIO sources, directly benefit hydraulics and water quality modellers, regulatory authorities, water resource managers and policy.

CRediT authorship contribution statement

Man Yue Lam: Conceptualization, Methodology, Software, Validation, Writing – original draft, Writing – review & editing. **Reza Ahmadian:** Conceptualization, Funding acquisition, Supervision, Writing – review & editing.

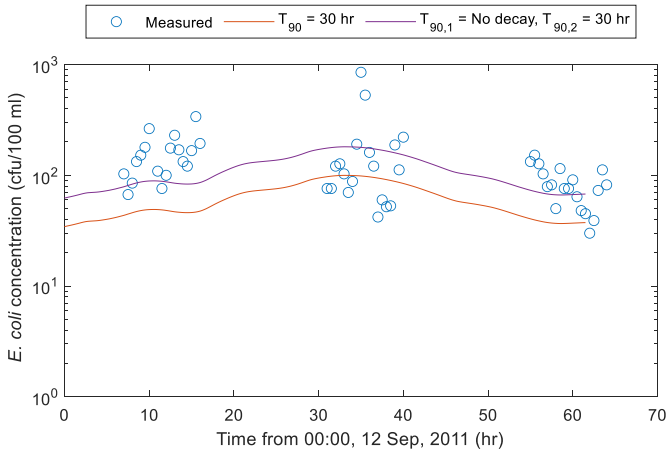

Fig. 7. Measured and hindcasted *E. coli* concentrations at the Swansea transect during 12–14 Sep 2011.

Declaration of competing interest

The authors declare that they have no known competing financial interests or personal relationships that could have appeared to influence the work reported in this paper.

Data availability

Numerical modelling data are available at request, but the authors do not have the permission to share field data used in this paper.

Acknowledgements

The study is carried out as a part of the EERES4WATER (Promoting Energy-Water nexus resource efficiency through renewable energy and energy efficiency) project, which is co-financed by the Interreg Atlantic Area Programme through the European Regional Development Fund under EAPA 1058/2018 and as a part of TidAl Range schemes as configurable Grid-scale Energy sTorage facilities (TARGET) under a grant from the Engineering and Physical Sciences Research Council (EPSRC), grant number EP/W027879/1.

Appendix A. Supplementary data

Supplementary data to this article can be found online at https://doi.org/10.1016/j.envpol.2024.123431.

References

Abu-Bakar, A., Ahmadian, R., Falconer, R.A., 2017. Modelling the transport and decay processes of microbial tracers in a macro-tidal estuary. Water Res. 123, 802–824.
Ahmadian, R., Falconer, R.A., Lin, B., 2010. Hydro-environmental modelling of proposed Severn barrage, UK. Proc. Inst. Civ. Eng.: Energy 163 (3), 107–117.
Ahmadian, R., Bomminayuni, S., Falconer, R.A., Stoesser, T., 2013. Numerical Modelling of Flow and Faecal Indicator Organism Transport at Swansea Bay, UK. A Report from the Interreg 4a Smart Coasts – Sustainable Communities Project.
Ahn, J.H., Grant, S.B., Surbeck, C.Q., Digiacomo, P.M., Nikolay, P., Nezlin, N.P., Jiang, S., 2005. Coastal water quality impact of stormwater runoff from an urban watershed in southern California. Environ. Sci. Technol. 39, 5940–5953.
Andruszkiewicz, E.A., Koseff, J.R., Fringer, O.B., Ouellette, N.T., Lowe, A.B., Edwards, C. A., Boehm, A.B., 2019. Modeling environmental DNA transport in the coastal ocean using Lagrangian particle tracking. Front. Mar. Sci. 6 article 477.
Bedri, Z., Bruen, M., Dowley, A., Masterson, B., 2013. Environmental consequences of a power plant shut-down: a three-dimensional water quality model of Dublin Bay. Mar. Pollut. Bull. 71, 117–128.

Bedri, Z., Corkery, A., O'Sullivan, J.J., Alvarez, M.X., Erichsen, A.C., Deering, L.A., Demeter, K., O'Hare, G.M.P., Meijer, W.G., Masterson, B., 2014. An integrated catchment-coastal modelling system for real-time water quality forecasts. Environ. Model. Software 61, 458–476.
Bedri, Z., Sullivan, J.J.O., Deering, L.A., Demeter, K., Masterson, B., Meijer, W.G., Harem, G.O., 2015. Assessing the water quality response to an alternative sewage disposal strategy at bathing sites on the east coast of Ireland. Mar. Pollut. Bull. 91 (1), 330–346.
British Crown and OceanWise Ltd, 2015. MCA 28 Bristol Channel (Wales). https://naturalresources.wales/evidence-and-data/maps/marine-character-areas/?lang=en. (Accessed 3 March 2023).
Bowie, G.L., Mills, W.B., Porcella, D.B., Campbell, C.L., Pagenkopf, J.R., Rupp, G.L., Johnson, K.M., et al., 1985. Rates, Constants, and Kinetics Formulations in Surface Water Quality Modeling. Environmental Research Laboratory, Office of Research and Development, U.S. Environmental Protection Agency, Athens, Georgia, 2nd edition.
Bussi, G., Whitehead, P.G., Thomas, A.R.C., Masante, D., Jones, L., Cosby, J.B., Emmett, B.A., Malham, S.K., Prudhomme, C., Prosser, H., 2017. Climate and land-use change impact on faecal indicator bacteria in a temperate maritime catchment (the River Conwy, Wales). J. Hydrology 553, 248–261.
Byappanahalli, M.N., Nevers, M.B., Korajkic, A., Staley, Z.R., Harwood, V.J., 2012. Enterococci in the environment. Microbiol. Mol. Biol. Rev. 76 (4), 685–706.
Chow, V.T., 1959. Open-channel Hydraulics. McGraw-Hill, New York.
Collins, M.B., Banner, F.T., 1980. Sediment transport by waves and tides: exemplified by a study of Swansea Bay, northern Bristol Channel. In: Banner, F.T., Collins, M.B., Massie, K.S. (Eds.), The Northwest European Shelf Seas: the Sea Bed and the Sea in Motion. 2. Physical and Chemical Oceanography and Physical Resources. Elsevier, pp. 369–389.
Crane, B.S., Moore, J.A., 1986. Modeling enteric bacterial die-off: a review. Water Air Soil Pollut. 27, 411–439.
DeFlorio-Barker, S., Wing, C., Jones, R.M., Dorevitch, S., 2018. Estimate of incidence and cost of recreational waterborne illness on United States surface waters. Environ. Health 17 (1) article 3.
European Commission, 2006. Directive 2006/7/EC of the European Parliament and of the Council of 15 February 2006 concerning the management of bathing water quality and repealing Directive 76/160/EEC. OJEU 64, 37–51.
Evans, G.P., Mollowney, B.M., Spoel, N.C., 1990. Two-dimensional modelling of the Bristol Channel, UK. In: Spaulding, M.L. (Ed.), Proceedings of the Conference on Estuarine and Coastal Modelling, pp. 331–340.
Ferrante, M., Brunone, B., 2003. Pipe system diagnosis and leak detection by unsteady-state tests. 1. Harmonic analysis. Adv. Water Resour. 26, 95–105.
Gaeta, M.G., Samaras, A.G., Archetti, R., 2020. Numerical investigation of thermal discharge to coastal areas: a case study in South Italy. Environ. Model. Software 124 article 104596.
Gao, G., Falconer, R.A., Lin, B., 2013. Modelling importance of sediment effects on fate and transport of Enterococci in the Severn Estuary, UK. Mar. Pollut. Bull. 67, 45–54.
Ge, Z., Whitman, R.L., Nevers, M.B., Phanikumar, M.S., 2012. Wave-induced mass transport affects daily Escherichia coli fluctuations in nearshore water. Environ. Sci. Technol. 46, 2204–2211.
Geyer, W.R., Signell, R.P., Fong, D.A., Wang, J., Anderson, D.M., Keafer, B.A., 2004. The freshwater transport and dynamics of the western marine coastal current. Continent. Shelf Res. 24, 1339–1357.
Given, S., Pendleton, L.H., Boehm, A.B., 2006. Regional public health cost estimates of contaminated coastal waters: a case study of gastroenteritis at southern California beaches. Environ. Sci. Technol. 40 (16), 4851–4858.
Gourgue, O., Baeyens, W., Chen, M.S., de Brauwere, A., de Brye, B., Deleersnijder, E., Elskens, M., Legat, V., 2013. A depth-averaged two-dimensional sediment transport model for environmental studies in the Scheldt Estuary and tidal river network. J. Mar. Syst. 128, 27–39.
Guo, B., Ahmadian, R., Evans, P., Falconer, R.A., 2020. Studying the wake of an island in a macro-tidal estuary. Water 12 (5), 1225.
Harris, E.L., Falconer, R.A., Lin, B., 2004. Modelling hydro-environmental and health risk assessment parameters along the South Wales Coast. J. Environ. Manag. 73, 61–70.
Hipsey, M.R., Antenucci, J.P., Brookes, D.J., 2008. A generic, process-based model of microbial pollution in aquatic systems. Water Resour. Res. 44, 1–26.
Huang, G., Falconer, R.A., Lin, B., 2015. Integrated river and coastal flow, sediment and Escherichia coli modelling for bathing water quality. Water (Basel) 7 (9), 4752–4777.
Huang, G., Falconer, R.A., Lin, B., 2018. Evaluation of E.coli Losses in a tidal river network using a refined 1-D numerical model. Environ. Model. Software 108, 91–101.
Isobe, A., Kako, S., Chang, P.H., Matsuno, T., 2009. Two-way particle-tracking model for specifying sources of drifting objects: application to the East China Sea shelf. J. Atmos. Ocean Tech. 26, 1672–1682.
Jalliffier-Verne, I., Leconte, R., Huaringa-Alvarez, U., Heniche, M., Madoux-Humery, A. S., Autixier, L., Galarneau, M., Servais, P., Prévost, M., Dorner, S., 2017. Modelling the impacts of global change on concentrations of Escherichia coli in an urban river. Adv. Water Resour. 108, 450–460.
Ji, Z., 2008. Hydrodynamics and Water Quality: Modeling Rivers, Lakes, and Estuaries. John Wiley & Sons Inc, New Jersey.
King, J., 2019. Investigation and prediction of pollution in coastal and estuarine waters, using experimental and numerical methods. PhD Thesis. Cardiff University, Cardiff, UK.
King, J., Ahmadian, R., Falconer, R.A., 2021. Hydro-epidemiological modelling of bacterial transport and decay in nearshore coastal waters. Water Res. 196 article 117049.
Lee, J.H.W., Qu, B., 2004. Hydrodynamic tracking of the massive spring 1998 red tide in Hong Kong. J. Environ. Eng., ASCE 130 (5), 535–550.
Leroy, A., 2019. *TELEMAC-3D Theory Guide*. TELEMAC-3D Documentation. EDF R&D, LNHE.
Limited, E.M.U., 2012. Swansea Bay Current Monitoring Operational Report. Technical report.
Liou, C.P., 1998. Pipeline leak detection by impulse response extraction. J. Fluid Eng. 120 (4), 833–838.
Liu, W.C., Chan, W.T., Young, C.C., 2015. Modeling fecal coliform contamination in a tidal Danshuei River estuarine system. Sci. Total Environ. 502, 632–640.
Mattioli, M.C., Sassoubre, L.M., Russell, T.L., Boehm, A.B., 2017. Decay of sewage-sourced microbial source tracking markers and fecal indicator bacteria in marine waters. Water Res. 108, 106–114.
Medeiros, S.C., Hagen, S.C., 2013. Review of wetting and drying algorithms for numerical tidal flow models. Int. J. Numer. Methods Fluid. 71, 473–487.
National Oceanography Centre Noc, 2018. Continental Shelf Model (CS3 and CS3-3D).
Ogata, K., 2015. Discrete-time control systems. In: 2nd and Indian Edition). Pearson India Education Service. Noida, India.
Pandey, P.K., Kass, P.H., Soupir, M.L., Biswas, S., Singh, V.P., 2014. Contamination of water resources by pathogenic bacteria. Amb. Express 4 article 51.
Passerat, J., Ouattara, N.K., Mouchel, J.M., Rocher, V., Servais, P., 2011. Impact of an intense combined sewer overflow event on the microbiological water quality of the Seine River. Water Res. 45, 893–903.
Perkins, T.L., Perrow, K., Rajko-Nenow, P., Jago, C.F., Jones, D.L., Malham, S.K., McDonald, J.E., 2016. Decay rates of faecal indicator bacteria from sewage and ovine faeces in brackish and freshwater microcosms with contrasting suspended particulate matter concentrations. Sci. Total Environ. 572, 1645–1652.
Pruss, A., 1998. Review of epidemiological studies on health effects from exposure to recreational water. Int. J. Epidemiol. 27 (4), 1–9.
Rogers, S.W., Donnelly, M., Peed, L., Kelty, C.A., Mondal, S., Zhong, Z., Shanks, O.C., 2011. Decay of bacterial pathogens, fecal Indicators, and real-time quantitative PCR genetic markers in manure-amended soils. Appl. Environ. Microbiol. 77 (14), 4839–4848.
Schippmann, B., Schernewhki, G., Grawe, U., 2013. Escherichia coli pollution in a Baltic Sea Lagoon: a model-based source and spatial risk assessment. Int. J. Hyg Environ. Health 216, 408–420.
Schnauder, I., Bockelmann-Evans, B., Lin, B., 2007. Modelling faecal bacteria pathways in receiving waters. Proc. Inst. Civ. Eng. Marit. Eng. 160, 143–154.
Schwarzenbach, J., Gill, K.F., 1992. System modelling and control. In: (3rd Edition). Edward Arnold, Hodder & Stoughton Publishers. Mill Road, Dunton Green, Sevenoaks, Kent.
Semadeni-Davies, A., Hernebring, C., Svensson, G., Gustafsson, L.G., 2008. The impacts of climate change and urbanisation on drainage in Helsingborg, Sweden: combined sewer system. J. Hydrol. 350, 100–113.
Smagorinski, J., 1963. General circulation experiments with the primitive equations. i. the basic experiment. Mon. Weather Rev. 91, 99–164.
Uncles, R.J., 1981. A numerical simulation of the vertical and horizontal M2 tide in the Bristol Channel and comparisons with observed data. Limnol. Oceanogr. 26, 571–577.
Varlamov, S.M., Yoon, J.H., Hirose, N., Kawamura, H., Shiohara, K., 1999. Simulation of the oil spill processes in the Sea of Japan with regional ocean circulation model. J. Mar. Sci. Technol. 4, 94–107.
Wang, X., Ghidaoui, M.S., Lee, P.J., 2020. Linear model and regularization for transient wave–based pipeline-condition assessment. J. Water Resour. Plann. Manage., ASCE 146 (5), 04020028.
Weiskerger, C.J., Phanikumar, M.S., 2020. Numerical modeling of microbial fate and transport in natural waters: review and implications for normal and extreme storm events. Water 12 (7), 1876 article.
Wyer, M.D., Kay, D., Watkins, J., Davies, C., Kay, C., Thomas, R., Porter, J., Stapleton, C. M., Moore, H., 2010. Evaluating short-term charges in recreational water quality during a hydrograph event using a combination of microbial tracers, environmental microbiology, microbial source tracking and hydrological techniques: a case study in southwest Wales, UK. Water Res. 44, 4783–4795.
Wyer, M.D., Kay, D., Morgan, H., Naylor, S., Govier, P., Clark, S., Watkins, J., Davies, C. M., Francis, C., Osborn, H., Bennett, S., 2013. Statistical Modelling of Faecal Indicator Organisms at a Marine Bathing Water Site: Results of an Intensive Study at Swansea Bay, UK, A Report from the Interreg 4a Smart Coasts – Sustainable Communities Project.
Wyer, M.D., Kay, D., Morgan, H., Naylor, S., Clark, S., Govier, P., Watkins, J., Davies, C. M., Francis, C., Jones, J.L., Palmer, C., Kay, C., 2014. Faecal indicator source connectivity for inputs to Swansea Bay. A report from the interreg 4a Smart Coast – Sustainable Communities project.
Wyer, M.D., Kay, D., Morgan, H., Naylor, S., Clark, S., Watkins, J., Davies, C.M., Francis, C., Osborn, H., Bennett, S., 2018. Within-day variability in microbial concentrations at a UK designated bathing water: implications for regulatory monitoring and the application of predictive modelling based on historical compliance data. Water Res. X 1 article 100006.
Zhang, Q., He, X., Yan, T., 2015. Differential decay of wastewater bacteria and change of microbial communities in beach sand and seawater microcosms. Environ. Sci. Technol. 49, 8531–8540.